

Effective field theory for distorted photonic crystals

Hitoshi Kitagawa,^{1,*} Kanji Nanjyo,¹ and Kyoko Kitamura^{1,2}

¹*Department of Electronics, Kyoto Institute of Technology, Matsugasaki, Sakyo-ku, Kyoto 606-8585, Japan*

²*Japan Science and Technology Agency, Precursory Research for Embryonic Science and Technology, 4-1-8 Honcho, Kawaguchi, Saitama 332-0012, Japan*



(Received 30 November 2020; revised 25 May 2021; accepted 25 May 2021; published 7 June 2021)

In this study, we used differential geometry to develop an effective field theory to study the behavior of light propagation in distorted photonic crystals (DPCs) of averagely homogeneous refractive index media. To study the light-ray trajectories in DPCs, we derived a geodesic equation based on the principle of least action by defining the metric tensor in terms of the lattice-position distortion. The geodesic equation implies that the lattice-position distortion can curve the trajectory. We present multiple exact solutions for the trajectory for simple distortion under the condition of having the same values of the lattice point filling factor at each unit cell. These solutions explicitly demonstrate that the light is only bent through the introduction of lattice distortion, and that these results are consistent with the finite-difference time-domain simulation results.

DOI: [10.1103/PhysRevA.103.063506](https://doi.org/10.1103/PhysRevA.103.063506)

I. INTRODUCTION

In recent years, differential geometry has been increasingly applied to describe physical phenomena. Einstein's geometrization philosophy for general relativity [1] is a classic example of the geometrization of physical laws by means of differential geometry. Transformation optics technologies [2–6] have also been developed based on differential geometry. In particular, Piwnicki studied the geometrical approach to an inhomogeneous medium [4]. In addition, there are close relationships between topological ideas and modern quantum field theory: for example, Berry phases, magnetic monopoles, Wess-Zumino terms, and skyrmions have been stated in the gauge theory [7]; the quantum Hall effect has been rearranged by means of topological indices [8,9]; and topological insulators and superconductors have been investigated with regards to topology [10].

Photonic crystals (PCs) have been studied as an arrangement of well-ordered periodic lattice points. The periodic structure facilitates the peculiar photonic dispersion that controls light behavior in various media. The modification of the lattice-point positions within a range that is narrower than the periodicity has also been applied to enhance existing nanocavity effects [11,12], or to add diffraction effects to the resonant mode [13,14]. There are also some precedent studies on PCs that consist of lattices without periodic structures (or breaking periodicity), where Newtonian mechanics was applied to wave packets of light to enhance the optical Hall effect [15,16]. Similarly, Deng *et al.* [17] reported a distorted photonic graphene structure in which the light is bent by the effective magnetic field produced by the Dirac point in the photonic band.

The main research question being addressed by this study is whether it is possible to bend propagating light in media with averagely homogeneous refractive index. To investigate this question, the key concepts of our hypothesis are as follows. The eigenstates of light in PCs are Bloch states. If random or steep fluctuations are applied, the Bloch states should be scattered. However, if the rate of fluctuations is sufficiently low, the Bloch states may be changed adiabatically. Based on this physical concept, we postulated that the regular structure reflects flat space-time, whereas the gradual changes of the structure reflect curved space-time. According to the theory of general relativity, gravity is a distortion of space-time caused by the presence of matter (or energy). Similarly, based on Fermat's principle, the framework of pseudogravity in inhomogeneous media has been developed in transformation optics [4–6]. Therefore, in this study, we investigate whether the pseudogravity is caused in a medium with an averagely homogeneous refractive index. Moreover, the above-mentioned pseudogravity can be represented using differential geometry. To the best of our knowledge, there are limited studies that apply differential geometry to PC structures.

In this paper, we discuss the characteristics of distorted photonic crystals (DPCs), i.e., the gradual spatial distortion that occurs in PC structures, from the perspective of differential geometry to elucidate the behavior of light passing through DPCs. Thus, we first construct an effective field theory for DPCs. Thereafter, we show that this field theory can be used to develop a geodesic equation to describe the trajectory of the light ray. We use a low-frequency region where the equifrequency contours are closed curves in order to not consider any peculiar photonic dispersion of photonic crystals. Finally, the exact solution is applied to simple examples and the results are compared to those of finite-difference time-domain (FDTD) simulations.

*Corresponding author: pamkitag@kit.ac.jp

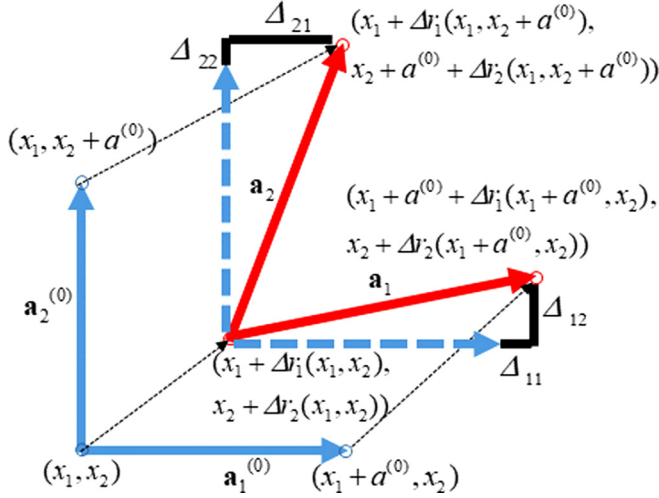


FIG. 1. Lattice distortion of a 2D square lattice. $\mathbf{a}_i^{(0)}$ ($i = 1, 2$) corresponds to the undistorted lattice vectors, and \mathbf{a}_i ($i = 1, 2$) corresponds to the distorted lattice vectors. $\Delta \mathbf{r}(\mathbf{x})$ is the lattice-point displacement. The lattice-distortion tensors ΔL_{ij} ($i, j = 1, 2$) were derived based on the deviation between $\mathbf{a}_i^{(0)}$ and \mathbf{a}_i .

II. EFFECTIVE FIELD THEORY FOR DISTORTED PHOTONIC CRYSTALS

A. Distortion tensor

In this study, we employ the long-wavelength approximation. Subsequently, we define the lattice-distortion tensors and assume the lattice vectors; therefore, the base vectors of the lattice correspond to the gradual function of space points. Considering the lattice-point displacements $\Delta \mathbf{r}(\mathbf{x})$ in a two-dimensional (2D) square lattice (Fig. 1), the diagonal elements of the lattice-distortion tensors are defined as

$$\begin{aligned} \Delta r_1(x_1 + a^{(0)}, x_2) - \Delta r_1(x_1, x_2) &\equiv \Delta L_{11}, \\ \Delta r_2(x_1, x_2 + a^{(0)}) - \Delta r_2(x_1, x_2) &\equiv \Delta L_{22}, \end{aligned} \quad (1)$$

Similarly, the off-diagonal elements of the lattice-distortion tensors were defined as

$$\begin{aligned} \Delta r_2(x_1 + a^{(0)}, x_2) - \Delta r_2(x_1, x_2) &\equiv \Delta L_{12}, \\ \Delta r_1(x_1, x_2 + a^{(0)}) - \Delta r_1(x_1, x_2) &\equiv \Delta L_{21}, \end{aligned} \quad (2)$$

where (x_1, x_2) is a position vector, and $a^{(0)}$ is the undistorted lattice constant.

Next, to consider the dielectric properties of the PC, we defined the distortion tensor, i.e., the renormalized lattice-distortion tensor Δ_{ij} , as

$$\Delta_{ij} \equiv \gamma \Delta L_{ij}. \quad (3)$$

Here, γ is the weight factor, which is defined as follows:

$$\gamma \equiv \left[\frac{\sum_{\mathbf{G} \neq 0} |\kappa(\mathbf{G})|^2}{(\sum_{\mathbf{G} \neq 0} |\kappa(\mathbf{G})|^2)^{\text{Max}}} \right]^{(0)} \frac{\sigma_P + 1}{2}, \quad (4)$$

$$\frac{1}{\varepsilon(\mathbf{r})} = \sum_{\mathbf{G}} \kappa(\mathbf{G}) \exp(i\mathbf{G} \cdot \mathbf{r}), \quad (5)$$

where $\sigma_P = 1$ for H polarization, $\sigma_P = -1$ for E polarization, $\varepsilon(\mathbf{r})$ is the periodic dielectric function, and \mathbf{G} is the reciprocal lattice vector of undistorted (or regular) PCs. Note that in this study, the dielectric constant of the medium was set at 3.5^2 . As detailed in the equations, γ contains the following information about undistorted PCs: the filling factor, dielectric contrast between the lattice point and background, and inclusion of the second-order perturbative corrections of the eigenvalues for PCs. Equation (4) also states that $\gamma = 0$ under the conditions of E polarization. This is because the E -polarized light is not affected by lattice distortion at long-wavelength frequencies.

B. Metric tensor

Our ansatz is that DPCs distort space-time in a way that can be observed by analyzing the light transmission. Therefore, we consider the metric tensor as a means to evaluate the space-time structure of DPCs. The relationship between $\mathbf{e}_i^{(0)}$ and \mathbf{e}_j ($i, j = 1, 2$) is represented in terms of the distortion tensors as follows:

$$\begin{bmatrix} \mathbf{e}_1 \\ \mathbf{e}_2 \end{bmatrix} = \begin{bmatrix} 1 + \Delta_{11}/a^{(0)} & \Delta_{12}/a^{(0)} \\ \Delta_{21}/a^{(0)} & 1 + \Delta_{22}/a^{(0)} \end{bmatrix} \begin{bmatrix} \mathbf{e}_1^{(0)} \\ \mathbf{e}_2^{(0)} \end{bmatrix}, \quad (6)$$

where $\mathbf{e}_i^{(0)}$ and \mathbf{e}_i ($i = 1, 2$) are the undistorted and distorted base vectors, respectively. The metric tensor of space was constructed by incorporating the sets of scalar products of the base vectors. Specifically, upon considering time and the refractive indices, the metric tensor ($g_{\mu\nu}$) of space-time was constructed as follows:

$$g_{\mu\nu} = \begin{bmatrix} -1 & 0 & 0 \\ 0 & (n^{(0)})^2 \{1 + 2(\Delta_{11}/a^{(0)} + \Delta n(\mathbf{x})/n^{(0)})\} & (n^{(0)})^2 (\Delta_{12} + \Delta_{21})/a^{(0)} \\ 0 & (n^{(0)})^2 (\Delta_{12} + \Delta_{21})/a^{(0)} & (n^{(0)})^2 \{1 + 2(\Delta_{22}/a^{(0)} + \Delta n(\mathbf{x})/n^{(0)})\} \end{bmatrix}, \quad (7)$$

where $n^{(0)}$ and $\Delta n(\mathbf{x})$ are the average and deviated refractive indices of the DPC, respectively; this metric tensor possesses all the geometric information about the DPC.

III. LIGHT PROPAGATION IN DISTORTED PHOTONIC CRYSTALS

A. Geodesic equation

Herein, we discuss the propagation of light in a DPC. We considered the trajectory of light by developing the geodesic

equation. The action S of a DPC is given by

$$S = \int \sqrt{-g_{\mu\nu} \frac{dx^\mu}{d\sigma} \frac{dx^\nu}{d\sigma}} d\sigma, \quad (8)$$

where σ is the arc length of the trajectory, and $\mu, \nu = 0, 1, 2$. Then, according to the principle of least

action,

$$\delta S = 0 \quad (9)$$

can be used to develop the geodesic equation

$$\frac{d^2 x^\mu}{d\tau^2} + \Gamma^\mu_{\nu\lambda} \frac{dx^\nu}{d\tau} \frac{dx^\lambda}{d\tau} = 0, \quad (10)$$

where $\Gamma^\mu_{\nu\lambda}$ is the connection coefficient given by the metric tensor of the DPC:

$$\Gamma^\mu_{\nu\lambda} = g^{\mu\tau} \frac{1}{2} (\partial_\lambda g_{\tau\nu} + \partial_\nu g_{\tau\lambda} - \partial_\tau g_{\nu\lambda}), \quad (11)$$

where $\lambda, \tau = 0, 1, 2$. The elements of the connection coefficient are given as follows:

$$\begin{aligned} \Gamma^0_{\nu\lambda} &= 0, \\ \Gamma^1_{11} &= \partial_1 \left(\frac{\Delta_{11}}{a^{(0)}} + \frac{\Delta n}{n^{(0)}} \right), \quad \Gamma^1_{12} = \partial_2 \left(\frac{\Delta_{11}}{a^{(0)}} + \frac{\Delta n}{n^{(0)}} \right), \\ \Gamma^1_{22} &= \partial_2 \left(\frac{\Delta_{12} + \Delta_{21}}{a^{(0)}} \right) - \partial_1 \left(\frac{\Delta_{22}}{a^{(0)}} + \frac{\Delta n}{n^{(0)}} \right), \\ \Gamma^2_{22} &= \partial_2 \left(\frac{\Delta_{22}}{a^{(0)}} + \frac{\Delta n}{n^{(0)}} \right), \quad \Gamma^2_{21} = \partial_1 \left(\frac{\Delta_{22}}{a^{(0)}} + \frac{\Delta n}{n^{(0)}} \right), \\ \Gamma^2_{11} &= \partial_1 \left(\frac{\Delta_{12} + \Delta_{21}}{a^{(0)}} \right) - \partial_2 \left(\frac{\Delta_{11}}{a^{(0)}} + \frac{\Delta n}{n^{(0)}} \right). \end{aligned} \quad (12)$$

B. Exact solutions for simple models

We consider the simple cases in which the local displacement $\Delta \mathbf{r}(\mathbf{x})$ is given as the quadratic function of the space points. In these cases, the geodesic equation provides exact solutions. Illustrations of the models and solutions are shown in Figs. 2(a) and 2(b). Figure 2(a) shows uniaxial distortion, and Fig. 2(b) shows biaxial distortion. To only consider the effects of lattice distortion, i.e., $\Delta n(\mathbf{x}) = 0$, we changed the radii $r^{(n)}$, $r^{(m,n)}$ in the direction of the distortion to ensure that all of the filling factors for the lattice point in the unit cell had the same values. The averaged refractive index (n_{av}) is homogeneous ($\Delta n(\mathbf{x}) = 0$). In the case of uniaxial (y-direction) distortion, the displacement $\Delta \mathbf{r}(\mathbf{x})$ is given by

$$\Delta \mathbf{r}(\mathbf{x})/a^{(0)} = (0, \beta(y/a^{(0)})^2), \quad (13)$$

where the constant β is a dimensionless distortion coefficient for the y direction. In this case, the geodesic equation is given by

$$\begin{aligned} \frac{d^2 x}{d\sigma^2} &= 0, \\ \frac{d^2 y}{d\sigma^2} &= -2\gamma\beta \left(\frac{dy}{d\sigma} \right)^2. \end{aligned} \quad (14)$$

The solution of these simultaneous differential equations, which yields the trajectory of the light ray input from the origin, is given by

$$y = \frac{1}{2\gamma\beta} \ln |(2\gamma\beta \tan \phi)x + 1|, \quad (15)$$

where the incident angle from the x axis is ϕ . Figure 2(c) shows the trajectories of the light ray in the cases of $\beta = \pm 0.006$. Note that the sign of β changes the bending direction.

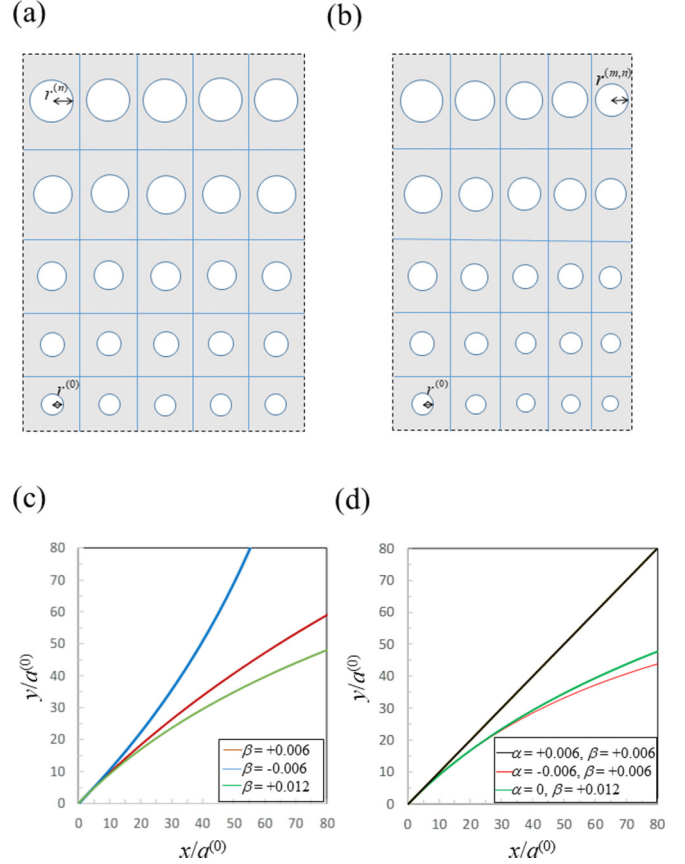


FIG. 2. Illustrations of example models and exact solutions. (a) Uniaxial distortion model. (b) Biaxial distortion model. (c, d) Light-ray trajectories in the case of uniaxial distortion and biaxial distortion, respectively. The incident angle, ϕ , from the x axis was $\pi/4$; the radius of the circular lattice point was set as $r^{(0)} = 0.4a^{(0)}$; $\Delta n(\mathbf{x}) = 0$. The brown (middle), blue (upper), and green (lower) curves of (c) correspond to $\beta = +0.006$, -0.006 , and $+0.012$, respectively. The black (upper) straight line of (d) corresponds to $\alpha = +0.006$ and $\beta = +0.006$, whereas the red (lower) curve of (d) corresponds to $\alpha = -0.006$ and $\beta = +0.006$, which yield a strong curve. The extent of curvature was very similar to that predicted for uniaxial distortion with double the β value [green (middle) curve].

In the case of biaxial distortion, the displacement $\Delta \mathbf{r}(\mathbf{x})$ is given by

$$\Delta \mathbf{r}(\mathbf{x})/a^{(0)} = (\alpha(x/a^{(0)})^2, \beta(y/a^{(0)})^2), \quad (16)$$

where α and β are the dimensionless distortion coefficients for the x and y directions, respectively. The geodesic equation is expressed as follows:

$$\begin{aligned} \frac{d^2 x}{d\sigma^2} &= -2\gamma\alpha \left(\frac{dx}{d\sigma} \right)^2, \\ \frac{d^2 y}{d\sigma^2} &= -2\gamma\beta \left(\frac{dy}{d\sigma} \right)^2. \end{aligned} \quad (17)$$

Then, the trajectory of the light ray is defined as follows:

$$y = \frac{1}{2\gamma\beta} \ln \left| \left(\frac{\beta}{\alpha} \tan \phi \right) (e^{2\gamma\alpha x} - 1) + 1 \right|. \quad (18)$$

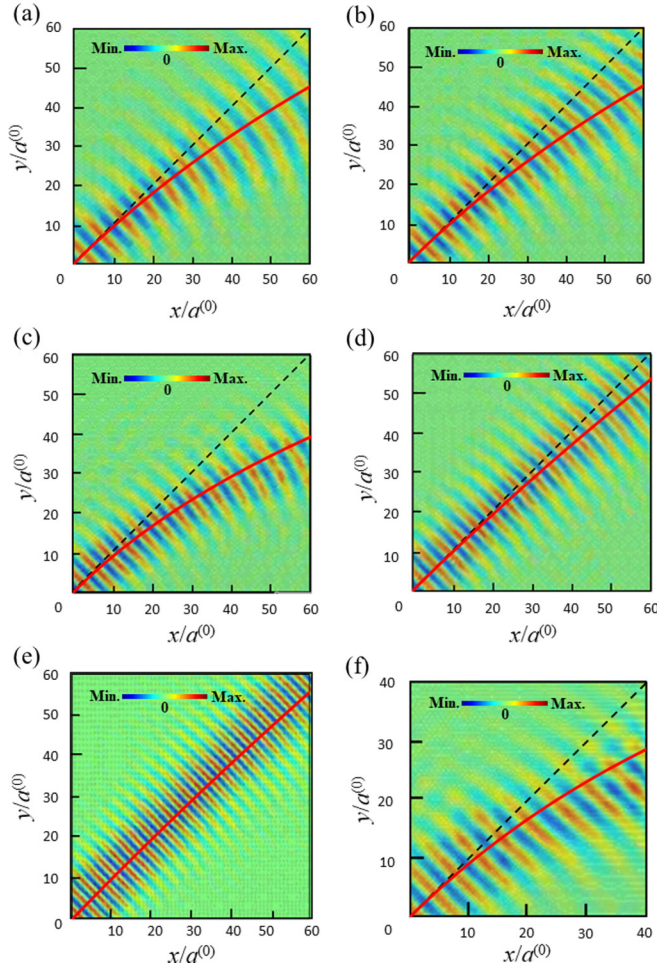


FIG. 3. Comparison of the theoretical and simulated results. The red curves represent the theoretical results, and the wavy field distributions show the results of FDTD simulation. $\Delta n(\mathbf{x}) = 0$ and $\phi = \pi/4$. (a–e) Uniaxial distortion results. The radius of the circular lattice point was set as $r^{(0)} = 0.4a^{(0)}$ for (a–c). (a) Air-hole lattice results for $\beta = +0.006$. (b) Dielectric-rod lattice results for $\beta = +0.006$. (c) Air-hole lattice results for $\beta = +0.01$. (d) Air-hole lattice results for $\beta = +0.002$. (e) Air-hole lattice results for $r^{(0)} = 0.2a^{(0)}$ and $\beta = +0.006$. (f) Biaxial distortion results for $\alpha = -0.006$, $\beta = +0.006$, and $r^{(0)} = 0.4a^{(0)}$.

The predicted light-ray trajectories in these cases are shown in Fig. 2(d). In the case of $\alpha = +0.006$ and $\beta = +0.006$, the trajectory is a straight line; in contrast, the conditions of $\alpha = -0.006$ and $\beta = +0.006$ yield a strongly curved trajectory. This curved trajectory is very similar to that corresponding to uniaxial distortion with twice the value of β .

IV. NUMERICAL EXPERIMENT

To verify our ansatz, we compared the aforementioned results to those of FDTD simulations. H polarization was applied in the FDTD simulation, and the normalized frequency was set to 0.1. It is worth mentioning that, in this study, we focused on the behavior of light without the influence of the Dirac point, in contrast to the study by Deng *et al.* [17], im-

plying that the long-wavelength approximation (normalized frequency of less than 0.1 approximately) is applicable.

Figure 3 shows a comparison of the results. The red line represents the theoretical results, and the wavy field distribution reflects the z component of the magnetic field in the simulation. We applied $\beta = +0.006$, $\phi = \pi/4$, and $r^{(0)} = 0.4a^{(0)}$. Although the beam divergence was slightly deviated, the theoretical results were consistent with the simulated results for the air-hole [Fig. 3(a)] and dielectric-rod [Fig. 3(b)] lattices. Increasing β to $+0.01$ resulted in a strongly curved trajectory [Fig. 3(c)]; conversely, reducing β significantly reduced the curvature of the trajectory [Fig. 3(d)]. Reducing $r^{(0)}$ to $0.2a^{(0)}$ also significantly reduced the curvature, with $r^{(0)} = 0$ tending toward a straight line [Fig. 3(e)]. These findings confirm that γ provides information about the PC. Even in the biaxial distortion case [Fig. 3(f)], the theoretical results are consistent with the simulated results. Thus, the ansatz presented in Sec. III is valid.

V. SUMMARY

From the perspective of differential geometry, we constructed an effective field theory to theoretically describe DPCs, which have been defined as PC structures that are subject to gradual spatial distortions. According to this theory, the trajectory of a light ray can be described by a geodesic equation that is similar to that for general relativity. Our results, which were derived under the condition that the averaged refractive index of a DPC is homogeneous, indicate that the trajectory of a light ray can be curved by only introducing lattice distortion. In this case, the source of pseudogravity in DPCs is described by the lattice distortions, while pseudogravity arises from the inhomogeneity of the medium in transformation optics. This finding was unexpected, considering Fermat's principle. This study presents a phenomenological low-energy (long-wavelength) effective field theory for DPCs, which is expected to contribute to the pseudogravity engineering applications in homogeneous optical media. However, the accuracy of this theory is not sufficient at high frequency, in particular, near the band-gap frequency, because long-wavelength approximation is not satisfied. As a side note, the light is not bent in the case of E polarization [$\sigma_p = -1$ in Eq. (4)] at low frequency, but is slightly affected by lattice distortion at high frequency. However, we have presented in this theory that light can be bent even if we have not used the peculiar photonic dispersion of photonic crystals.

ACKNOWLEDGMENTS

This work was supported by JST, PRESTO Grant No. JP20345471, Japan. We are also grateful to Professor S. Iwamoto, Dr. Y. Ota, Dr. Y. Nakata, Dr. M. Fujita, and Professor S. Noda for their valuable contributions to the discussions.

APPENDIX

In the main text, we only applied $\Delta n(\mathbf{x}) = 0$ to focus solely on the effects of lattice distortion. However, the influence of

$\Delta n(\mathbf{x})$ can be investigated by setting the radii of all lattice points as constant. A similar case has already been reported by Deng *et al.* [17]; they concluded that effective magnetic field bends the light trajectory. However, in our viewpoint, their results include both effects of effective magnetic field and pseudogravity, because their structure is inhomogeneous media as follows. In the uniaxial distortion case, the geodesic equations become

$$\begin{aligned}\frac{d^2x}{d\sigma^2} &= -2\partial_y\left(\frac{\Delta n}{n^{(0)}}\right)\left(\frac{dx}{d\sigma}\right)\left(\frac{dy}{d\sigma}\right), \\ \frac{d^2y}{d\sigma^2} &= -2\gamma\beta\left(\frac{dy}{d\sigma}\right)^2 + \left[\left(\frac{dx}{d\sigma}\right)^2 - \left(\frac{dy}{d\sigma}\right)^2\right]\partial_y\left(\frac{\Delta n}{n^{(0)}}\right),\end{aligned}\quad (\text{A1})$$

where $\beta > 0$. Here, we set

$$\partial_y\left(\frac{\Delta n}{n^{(0)}}\right) \equiv \gamma\alpha', \quad (\text{A2})$$

and assume that

$$\alpha' \cong \alpha \quad (\text{A3})$$

and

$$\phi \cong \pi/4. \quad (\text{A4})$$

Then, incorporating Eq. (A4) results in the following:

$$\begin{aligned}\left(\frac{dx}{d\sigma}\right) &\cong \left(\frac{dy}{d\sigma}\right), \\ \left(\frac{dx}{d\sigma}\right)\left(\frac{dy}{d\sigma}\right) &\cong \left(\frac{dx}{d\sigma}\right)^2, \\ \left(\frac{dx}{d\sigma}\right)^2 - \left(\frac{dy}{d\sigma}\right)^2 &\cong 0,\end{aligned}\quad (\text{A5})$$

which yields

$$\frac{d^2x}{d\sigma^2} \cong -2\gamma\alpha\left(\frac{dx}{d\sigma}\right)^2, \quad \frac{d^2y}{d\sigma^2} \cong -2\gamma\beta\left(\frac{dy}{d\sigma}\right)^2. \quad (\text{A6})$$

These equations are similar to those corresponding to the biaxial distortion case of $\Delta n(\mathbf{x}) = 0$. The trajectory is also given by

$$y \cong \frac{1}{2\gamma\beta} \ln \left| \left(\frac{\beta}{\alpha} \tan \phi \right) (e^{2\gamma\alpha x} - 1) + 1 \right|. \quad (\text{A7})$$

Based on Eqs. (A2) and (A3), if the lattice points are air holes, then $\alpha < 0$, but if the lattice points correspond to a dielectric rod, then $\alpha > 0$. Thus, for an air-hole lattice, $\alpha > 0$ and $\beta > 0$; these conditions yield similar results to those shown by the black line in Fig. 2(d), which shows minimal curvature of the light trajectory. Alternatively, under the conditions of a dielectric-rod lattice, $\alpha < 0$ and $\beta > 0$; these conditions yielded a similar result to that shown by the red line in Fig. 2(d), which shows a strongly curved light-ray trajectory. The above-mentioned case is consistent with the results of Ref. [17].

-
- [1] A. Einstein, The foundation of the general theory of relativity, *Ann. Phys. (Berlin)* **354**, 769 (1916).
 - [2] U. Leonhardt, Optical conformal mapping, *Science* **312**, 1777 (2006).
 - [3] J. B. Pendry, D. Schurig, and D. R. Smith, Controlling electromagnetic fields, *Science* **312**, 1780 (2006).
 - [4] P. Piwnicki, Geometrical approach to light in inhomogeneous media, *Int. J. Mod. Phys. B* **17**, 1543 (2002).
 - [5] T. G. Philbin, C. Kuklewicz, S. Robertson, S. Hill, S. Konig, and U. Leonhardt, Fiber-optical analog of the event horizon, *Science* **319**, 1367 (2008).
 - [6] U. Leonhardt and P. Piwnicki, Optics of nonuniformly moving media, *Phys. Rev. A* **60**, 4301 (1999).
 - [7] A. Shapere and F. Wilczek, *Geometric Phases in Physics* (World Scientific, Singapore, 1989).
 - [8] S. C. Zhang, The Chern-Simons-Landau-Ginzburg theory of the fractional quantum Hall effect, *Int. J. Mod. Phys. B* **06**, 25 (1992).
 - [9] D. J. Thouless, M. Kohmoto, M. P. Nightingale, and M. den Nijs, Quantized Hall Conductance in a Two-Dimensional Periodic Potential, *Phys. Rev. Lett.* **49**, 405 (1982).
 - [10] X. L. Qui and S. C. Zhang, Topological insulators and superconductors, *Rev. Mod. Phys.* **83**, 1057 (2011).
 - [11] Y. Akahane, T. Asano, B.-S. Song, and S. Noda, High-Q photonic nanocavity in a two-dimensional photonic crystal, *Nature (London)* **425**, 944 (2003).
 - [12] B.-S. Song, S. Noda, T. Asano, and Y. Akahane, Ultra-high-Q photonic double-heterostructure nanocavity, *Nat. Mater.* **4**, 207 (2005).
 - [13] S. Noda, K. Kitamura, T. Okino, D. Yasuda, and Y. Tanaka, Photonic-crystal surface-emitting lasers: Review and introduction of modulated-photonic crystals, *IEEE J. Sel. Top. Quantum Electron.* **23**, 4900107 (2017).
 - [14] K. Kitamura, T. Okino, D. Yasuda, and S. Noda, Polarization control by modulated photonic-crystal lasers, *Opt. Lett.* **44**, 4718 (2019).
 - [15] M. Onoda, S. Murakami, and N. Nagaosa, Geometrical aspects in optical wave-packet dynamics, *Phys. Rev. E* **74**, 066610 (2006).
 - [16] K. Sawada, S. Murakami, and N. Nagaosa, Dynamical Diffraction Theory for Wave Packet Propagation in Deformed Crystals, *Phys. Rev. Lett.* **96**, 154802 (2006).
 - [17] F. Deng, Y. Li, Y. Sun, X. Wang, Z. Guo, Y. Shi, H. Jiang, K. Chang, and H. Chen, Valley-dependent beams controlled by pseudomagnetic field in distorted photonic graphene, *Opt. Lett.* **40**, 3380 (2015).